Available online at www.sciencedirect.com
SCIENCE DIRECT®
Polymer 44 (2003) 6927–6936
polymer
www.elsevier.com/locate/polymer

# Fast-responsive semi-interpenetrating hydrogel networks imaged with confocal fluorescence microscopy

Marianne E. Harmon[a], Wolfgang Schrof[b], Curtis W. Frank[a,*]

[a]*Department of Chemical Engineering, Stanford University, 381 North–South Mall, Stanford, CA 94305-5025, USA*
[b]*Polymer Physics, BASF Aktiengesellschaft, Ludwigshafen 67056, Germany*

Received 12 May 2003; received in revised form 25 July 2003; accepted 28 July 2003

**Abstract**

The composition of semi-interpenetrating polymer networks (semi-IPNs) based on responsive *N*-isopropylacrylamide (NIPAAm) hydrogels has been shown to affect the kinetics of the volume phase transition. Several *N*-alkyl-substituted acrylamides were used as the linear polymers in a crosslinked NIPAAm network, and the kinetics was observed as a function of crosslinking density and linear polymer concentration. The time required for collapse of the network could be reduced by as much as 90%, with little change to the corresponding swelling ratio and volume phase transition temperature. However, the underlying changes in network morphology are not known, and here we present kinetics data in combination with imaging of the resulting hydrogel networks. The crosslinked networks and the linear polymers were fluorescently labeled, and the resulting morphology was imaged with confocal fluorescence microscopy and two-photon laser scanning microscopy. The most hydrophilic of the linear polymers was acrylamide, which was shown to phase separate during polymerization. The hydrophilic domains become more interconnected at higher concentrations of the crosslinker and the linear polymers. This correlates well with the kinetics of the volume phase transition for the corresponding networks. The semi-IPNs containing more hydrophobic linear polymers had very similar morphology, but some domains were present, ranging from 500 nm to 2 μm and increasing in size with increased linear polymer concentration. The time scale of collapse was an order of magnitude faster than expected, based on size of the hydrophobic *N*-alkyl group, when the linear polymer had the same lower critical solution temperature as the hydrogel network. This is an indication that the simultaneous collapse of the linear polymer and the crosslinked network contributes to the fast response of these semi-IPNs.


*Keywords:* Responsive hydrogels; Semi-IPNs; Confocal microscopy

## 1. Introduction

The volume phase transition of hydrogels can be triggered by a number of different stimuli, including temperature [1], pH [2], electric field [3], light [4], and stress [5]. The polymer undergoes a collapse from an extended coil to a globular structure, a transition revealed on the macroscopic scale by a sudden decrease in the degree of swelling of the crosslinked gels. The large volume changes and the biocompatibility of many hydrogels have resulted in a wide range of applications in biomaterials [6] and drug delivery [7]. One of the most intensively studied polymers in this field is poly(*N*-isopropylacrylamide) (NIPAAm), which exhibits a sharp phase transition in water upon heating above 32 °C [8]. However, the kinetics of the volume phase transition is often a limiting factor, and the rate of collapse scales with the square of the gel size [9]. The rate of response has been accelerated through reducing the size of the gel [10,11], producing macroporous or inhomogeneous gels [12–15], and grafting hydrophilic or responsive polymers into the network [16,17]. Hydrogels have also been imaged with atomic force microscopy [18,19], scanning electron microscopy [20,21], and confocal fluorescence microscopy [22,23] and are known to have a spongy or microporous structure.

Interpenetrating polymer networks (IPNs), which consist of both linear and crosslinked polymers that are polymerized simultaneously or sequentially, have been used to improve the properties of polymer blends and composites [24]. IPNs and semi-IPNs based on hydrogels have been used for tissue engineering and drug delivery [25–27], and the network can consist of chemical or physical crosslinks [24]. Hydrophilic [28], responsive [29], and biocompatible

* Corresponding author. Tel.: +1-650-723-4573; fax: +1-650-723-9780.
*E-mail address:* curt.frank@stanford.edu (C.W. Frank).

0032-3861/$ - see front matter © 2003 Elsevier Ltd. All rights reserved.
doi:10.1016/j.polymer.2003.07.006

[27,30] functional groups can be incorporated into a semi-IPN, and the ability to independently vary the crosslinked and linear components provides a versatile platform. When the crosslinked network is responsive, the semi-IPN retains the responsive behavior of the crosslinked component as long as the linear polymer is not strongly ionized or hydrogen bonded with the crosslinked network [31,32]. The addition of hydrophilic and responsive linear polymers has also been shown to affect the kinetics of the volume phase transition [33,34].

Previous analyses of the kinetics of the responsive semi-IPN volume phase transition have assumed that the linear polymer is uniformly distributed [34] and trapped within the network [33], although extraction experiments have shown that the linear polymer also acts as a porogen [30,34]. Structures of IPNs and semi-IPNs have been studied by scattering [35] and scanning electron microscopy [20], but this does not allow the linear and crosslinked components to be studied independently. A more quantitative interpretation of these data in terms of overlap and interpenetration of the linear polymers can be found in Ref. [34]. Here we present a more qualitative approach, using confocal fluorescence microscopy and fluorescent labeling to separately image the linear and crosslinked components of responsive semi-IPNs based on NIPAAm. The kinetics of the volume phase transition of these semi-IPNs is known to vary with changes in the crosslinked and linear components, but the underlying structure of the resulting network is not known.

Our objective is to present both kinetic data and images of the hydrogel morphology so that the network structure can be correlated with the response to a step change in temperature. We have considered the effects of the linear polymer concentration and the crosslinking density of the crosslinked network. Several different linear polymers were used to study the effects of varying hydrophilicity, molecular weight, and lower critical solution temperature (LCST).

## 2. Experimental section

### 2.1. Materials

*N*-Isopropylacrylamide (NIPAAm; Aldrich) was recrystallized from *n*-hexane, and *N*,*N*-dimethylacrylamide (DMAAm; Aldrich) and *N*,*N*-diethylacrylamide (DEAAm; Polysciences, Inc.) were distilled under vacuum to remove inhibitor. *N*-Methylacrylamide (MAAm; ABCR), *N*-ethylacrylamide (EAAm; ABCR), acrylamide (AAm; Life Technologies), ammonium persulfate (APS; Aldrich), *N*,*N*′-methylenebisacrylamide (BIS; Aldrich), *N*,*N*,*N*′,*N*′-tetramethylethylenediamine (TEMED; Aldrich), γ-methacryloxypropyltrimethoxysilane (Sigma), allylamine (Aldrich), fluorescein-5-isothiocyanate (Molecular Probes), rhodamine B isothiocyanate (Polysciences), and fluorescein dimethacrylate (Polysciences) were of the highest available purity and were used as received.

### 2.2. Synthesis of linear polymers

Seven hundred mM monomer and 6 μl/ml TEMED were dissolved in water. The solution was bubbled with nitrogen and 0.4 mg/ml APS was added to initiate the reaction. Lower molecular weight polymers were synthesized as above except 0.8 mg/ml APS was added. The molecular weight of the polymer was calculated using intrinsic viscosity measurements [36], which are shown in Table 1, and the monomers used for the linear polymers are shown in Scheme 1. Copolymers of NIPAAm and AAm were also synthesized with the AAm concentration varying from 1 to 10 mol%, and these copolymers are referred to as NIPAAm-*co*-AAm followed by the mol% of AAm (for example, NIPAAm-*co*-AAm5). The NIPAAm and DEAAm polymers and the NIPAAm-*co*-AAm copolymers each exhibited an LCST, which was measured by differential scanning calorimetry [11]; these values are shown in Table 1. LCST behavior has also been reported for EAAm around 70 °C [37], but all experiments in this study are at temperatures at 50 °C or below, so in this case we do not consider EAAm to be a responsive polymer. The fluorescently labeled linear polymers were synthesized as above, except for the addition of 0.1% allylamine monomer. The resulting polymer was fluorescently labeled with fluorescein-5-isothiocyanate or rhodamine B isothiocyanate using standard methods [38]. The molecular weights and LCSTs of the fluorescently labeled linear polymers were within the standard deviations of the corresponding unlabeled polymers.

### 2.3. Synthesis of semi-IPNs

Each sample contains NIPAAm as the crosslinked component with different polymers as the linear component. Therefore, the naming convention used here is to label the samples according to the corresponding linear component. Bulk semi-IPNs were cast in a cylindrical shape, and these samples were used to study the kinetics of the volume phase transition. NIPAAm monomer (700–600 mM), linear

Table 1
Characterization of linear polymers

| Sample | High MW (g/mol) | Low MW (g/mol) | LCST (°C) |
|---|---|---|---|
| Aam | 600,000 | 500,000 | |
| MAAm | 1,000,000 | | |
| DMAAm | 300,000 | | |
| EAAm | 400,000 | | |
| NIPAAm | 500,000 | 300,000 | 32 |
| NIPAAm-*co*-AAm1 | 500,000 | | 33 |
| NIPAAm-*co*-AAm2 | 500,000 | | 34 |
| NIPAAm-*co*-AAm5 | 600,000 | | 36 |
| NIPAAm-*co*-AAm10 | 500,000 | | 40 |
| DEAAm | 200,000 | | 25 |

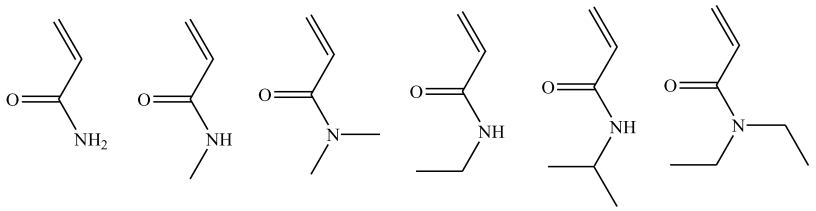


Scheme 1. Monomers used for linear polymer synthesis.

polymer (0–100 mM), BIS (0.5–2.1 mol%) and TEMED (6 μl/ml) were dissolved in water. The total network concentration was kept constant with the sum of the NIPAAm monomer and linear polymer equaling 700 mM. The pre-gel solution was poured into a test tube containing glass capillaries (inside diameter 0.95 mm), the solution was bubbled with nitrogen, and 0.4 mg/ml APS was added to initiate the reaction. After 24 h, the gels were removed from the capillaries and allowed to equilibrate in a large volume of MilliQ water to remove any unreacted reagents. The resulting cylindrical gels were used for the kinetics experiments. The equilibrium swelling ratio of the cylindrical gels as a function of temperature was also measured with both labeled and unlabeled linear polymers.

Bulk semi-IPNs were also polymerized on cover slips, and these samples were used for confocal fluorescence microscopy imaging of the network structure. These semi-IPNs were fluorescently labeled and prepared as described above, but a small droplet of the pre-gel solution was placed on a microscope cover slip that had been treated with γ-methacryloxypropyltrimethoxysilane, which forms a covalent bond between the cover slip and the gel [39]. The reaction was allowed to proceed for 24 h in a water-saturated nitrogen atmosphere. For double-staining experiments, fluorescein dimethacrylate was substituted for 1% of the BIS crosslinker, and the linear polymer was labeled with rhodamine B isothiocyanate. All other samples used linear polymer labeled with fluorescein-5-isothiocyanate.

### 2.4. Kinetics experiments

Each cylindrical gel sample was placed in a water-filled sample holder, and the diameter of the gel was observed using an optical microscope with an Instec HCS400-STC200 stage to control the temperature. The change in diameter was observed in response to step changes in temperature. The temperature was changed from 22 to 50 °C for deswelling experiments and from 50 to 22 °C for swelling experiments. Because the time required for the change in temperature was approximately 10 s, the first data point was taken at 10 s.

### 2.5. Confocal fluorescence microscopy

Two-photon laser scanning microscopy was used for 3D imaging of fluorescently labeled semi-IPNs. Femtosecond pulses to induce two-photon absorption and subsequent fluorescence emission were generated by a Ti:sapphire laser (Mira 900F, Coherent) pumped by an Ar ion laser (Innova 200, Coherent). The laser pulses were coupled to the microscope (DM IRBE microscope, TCS SP confocal scanning head, Leica Microsystems) through an optical fiber. A pulse stretcher (grating) and post-fiber compressor unit resulted in laser pulses at the focus of the microscope objective being Fourier transform limited with pulse widths of approximately 120 fs and a wavelength tunable from 750 to 850 nm.

The laser scanning microscope was also equipped with a prism spectrometer in the detection pathway, and available one-photon excitation wavelengths were 458, 488, 576, and 633 nm. Three photomultiplier detectors could be operated with optical bandwidths individually adjusted for spectral position and width, and this was used for double-staining experiments using a combination of rhodamine B and fluorescein. Spatial resolution of approximately 200 nm laterally and 400 nm axially could be achieved.

The two confocal microscopy techniques vary in resolution, the amount of photobleaching, and the number of fluorophores that can be used. Two-photon laser scanning microscopy has lower resolution, but the reduced photobleaching enhances the capacity for 3D imaging. Conventional (one-photon) confocal fluorescence microscopy has higher resolution and can use multiple fluorophores simultaneously for double-staining experiments, but with significant photobleaching above and below the plane of focus, it is best used for 2D images.

## 3. Results

### 3.1. Semi-IPNs

Crosslinked NIPAAm hydrogels have a volume phase transition that corresponds to the LCST of linear NIPAAm polymer. However, the kinetics of this volume phase transition is often a limiting factor in applications of these materials. The large friction between the solvent and the polymer network slows the diffusion of water within the gel network. The network also undergoes a non-uniform collapse, forming a dense hydrophobic layer at the surface

which further slows the diffusion of water from the core of the gel. Semi-IPNs based on NIPAAm as the crosslinked component and poly(acrylamide) as the linear component [33] and comb-grafted NIPAAm and poly(ethylene glycol) (PEG) oligomers in the NIPAAm network [16,17] have exhibited accelerated collapse of the gel network. The hydrophilic PEG oligomers are thought to act by providing water release channels, which facilitate the diffusion of water through the hydrophobic surface layer. The responsive NIPAAm oligomers allow rapid hydrophobic aggregation throughout the network and a more uniform network collapse, which reduces the formation of the hydrophobic surface layer [40]. The same mechanism is likely for the linear component of semi-IPNs based on NIPAAm, and we will apply this to the data analysis in the subsequent sections.

Here we use semi-IPNs based on NIPAAm as the crosslinked component and a series of *N*-alkyl-substituted acrylamides (see Scheme 1) as the linear component. Again, since the crosslinked component is the same for all the semi-IPNs, we refer to the samples according to the linear component. The NIPAAm and DEAAm linear polymers are thermally responsive, exhibiting LCST behavior, and by increasing the size of the *N*-alkyl group, the linear component becomes more hydrophobic. Therefore, the relative effects of the hydrophilic and responsive linear polymers can be studied in more detail. To quantify the relative sizes of the hydrophobic groups, the volume of each monomer and the volume of the *N*-alkyl group were calculated with ChemOffice. The percentage of the monomer volume that constitutes the hydrophobic *N*-alkyl group was used to estimate the relative hydrophobic and hydrophilic nature of the different monomers, and these values are shown in Table 2.

The linear polymers in these systems have been described as porogens [34] and as being activated by chain transfer and subsequently trapped during the gel polymerization process [33]. The samples are placed in water to leach out any unreacted reagents or linear polymer, and somewhere between 60 and 80% of the linear polymer does diffuse out of the network [34]. The diffusion coefficients from these measurements suggest that the resulting network has an open and porous structure. Thus, the semi-IPN samples contain NIPAAm as the crosslinked component along with trapped linear polymers that were activated during the gel polymerization and a porous structure from the linear polymers that have diffused out of the system. However, the leaching process does not affect the kinetics of the volume phase transition for the resulting samples [34], which suggests that the rate of response is primarily determined by the linear polymers that remain trapped in the network.

Table 2
Relative size of hydrophobic *N*-alkyl group

| Monomer | % of monomer volume |
|---|---|
| Aam | 0.0 |
| MAAm | 18.2 |
| DMAAm | 31.5 |
| EAAm | 32.4 |
| NIPAAm | 41.4 |
| DEAAm | 49.2 |

### 3.2. Kinetics of the volume phase transition

Several reference experiments were used to determine the range of linear polymer concentrations to be used. The equilibrium diameter of the cylindrical semi-IPNs was tracked as a function of temperature for samples containing different concentrations of linear polymer, and the equilibrium swelling ratio and transition temperature were found to be determined primarily by the degree of crosslinking. The presence of different chromophores and the type or concentration of the linear polymer did not affect the equilibrium swelling as long as the linear polymer concentration was not above 100 mM. Therefore, all kinetics measurements were for samples with linear polymer concentrations ranging from 0 to 100 mM. This is consistent with previous measurements on responsive semi-IPNs, such that the linear polymer is only expected to affect the transition temperature and the equilibrium swelling ratio if it is strongly ionized or hydrogen bonded with the crosslinked network [31,32]. The confocal fluorescence microscopy imaging requires that the network be fluorescently labeled, and it is assumed that the morphology is not affected by the fluorescent probe. Reference experiments were also used to verify that the presence of the chromophores did not affect the kinetics of the volume phase transition, but all the kinetics data is presented for unlabeled semi-IPNs.

Linear polymers do not affect the swelling ratio of the semi-IPN, but when the same samples undergo a step change in temperature, the rate of collapse is affected by the linear polymers trapped in the network. The diameter of the cylindrical gel is tracked as a function of time (see Fig. 1), and the rate of collapse is approximated by fitting this with a single exponential ($\sim \exp[-t/\tau]$). The characteristic time scale $\tau$ is a function of the type and concentration of linear polymer as well as the crosslinking density of the crosslinked network. AAm is unique in that it exhibits a non-monotonic effect of linear polymer concentration on $\tau$ (see Fig. 1). All other samples show a monotonic effect of linear polymer concentration on $\tau$, and we have looked at the response of the two fastest samples (AAm and NIPAAm) in greater detail.

As a result of the non-monotonic effect of linear AAm polymer concentration, $\tau$ goes through a maximum at low concentrations, followed by a decrease at higher concentrations, as shown in Fig. 2A. The location of the maximum and the rate of decrease at higher concentrations is a function of the crosslinking density, with faster response at higher crosslinking densities. This is compared to the

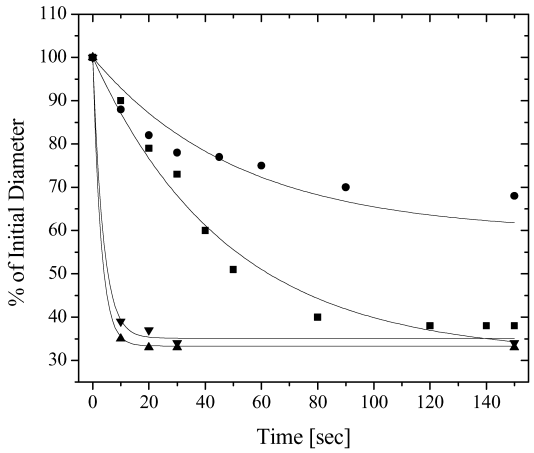


Fig. 1. The diameter of the cylindrical semi-IPN as a function of time in response to a step change in temperature from 22 to 50 °C. The concentrations of linear polymer are 0 mM (■), 30 mM (●), 70 mM (▼), and 100 mM (▲) with a crosslinker concentration of 2.1% BIS. The initial diameters of these samples are around 1 mm but vary slightly with the linear polymer concentration. The solid lines are fits to a single exponential ($\sim \exp[-t/\tau]$).

response of NIPAAm samples, shown in Fig. 2B, where $\tau$ decreases monotonically with the concentration of linear NIPAAm chains, also with faster response at higher crosslinking densities. Furthermore, the two sets of samples are different in the effect of molecular weight on the kinetics. The AAm samples are faster with higher molecular weight linear polymer, while the NIPAAm samples are faster with lower molecular weight linear polymer. If the linear polymers are uniformly distributed, this might be explained in terms of greater overlap of the hydrophilic water release channels for the higher molecular weight AAm samples and faster mobility of the linear NIPAAm chains for the lower molecular weight NIPAAm samples. However, by using confocal fluorescence microscopy, we can consider the relative mobility and overlap of the linear polymers as well as observing the effects on the semi-IPN morphology.

Fig. 3 shows $\tau$ as a function of the linear polymer used, in order of increasing hydrophobicity, using the estimates from Table 2. The time scale clearly increases with increasing size of the hydrophobic group, with the exception of NIPAAm. In this case, the linear and crosslinked components of the semi-IPN are the same, and the two components will respond simultaneously to the step change in temperature. The cooperative motion as the linear and crosslinked components collapse simultaneously may be responsible for the fast rate of response for this particular sample.

A series of semi-IPNs, varying the LCST of the linear component while keeping the crosslinked component constant, were used to test the effect of this simultaneous collapse on the time scale of response. The linear polymers were copolymers of NIPAAm and AAm (1–10 mol%), and the LCST increased with increasing AAm concentration

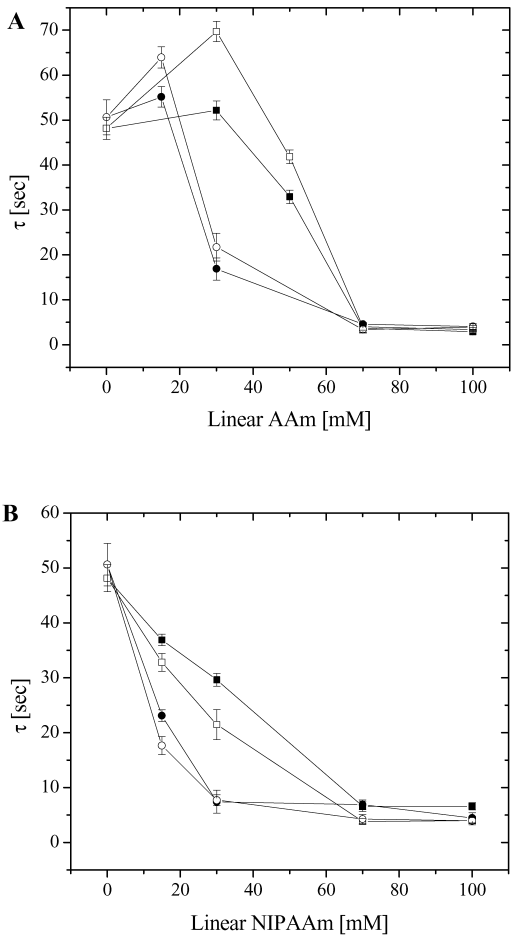


Fig. 2. The time scale $\tau$ for (A) AAm and (B) NIPAAm semi-IPNs as a function of linear polymer concentration for crosslinked networks with 1.2% BIS (■, □) and 2.1% BIS (●, ○). The samples contain either high (solid symbols) or low (open symbols) molecular weight linear polymers, as shown in Table 1.

(see Table 1) [41]. The crosslinked NIPAAm network has an LCST of 32 °C, and $\tau$ increased with increasing LCST of the linear polymer (see Fig. 4). When the linear and crosslinked

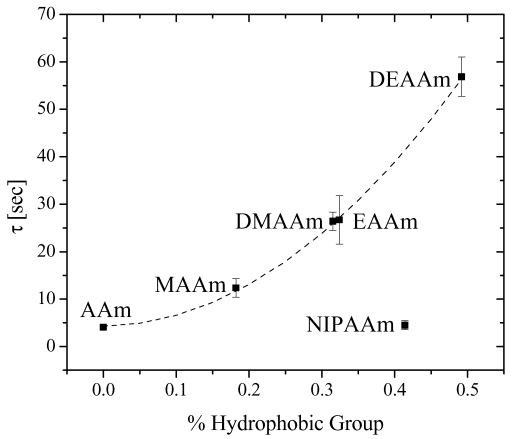


Fig. 3. The time scale $\tau$ as a function of the *N*-alkyl group size for the corresponding monomer, as listed in Table 2. Samples are 100 mM of the linear polymer with a crosslinker concentration of 2.1% BIS.

components have different transition temperatures, they do not respond simultaneously, and this supports the idea that the responsive linear polymers act through cooperative motion and uniform collapse of the resulting network. Fig. 3 also includes a data point where the linear polymer (DEAAm, 25 °C) has an LCST lower than that of the crosslinked network, and we will compare these sets of samples in Section 4.

### 3.3. Confocal imaging of the semi-IPNs

Two-photon laser scanning microscopy was used for imaging of samples with fluorescein-labeled AAm and NIPAAm linear polymers as a function of linear polymer concentration and crosslinking density. This technique is similar to confocal fluorescence microscopy, but because of the two-photon effect, it does not photobleach the sample above and below the plane of focus, which facilitates 3D imaging of the semi-IPNs. The AAm samples (see Fig. 5) have distinct regimes of high and low linear AAm concentration that become more interconnected with increasing crosslinking density and linear polymer concentration. The interconnected hydrophilic domains correspond to faster rate of response, and the separate domains at low concentrations correspond to the maximum in $\tau$ as shown in Fig. 2A. The NIPAAm samples (see Fig. 6) have regions of higher and lower linear NIPAAm concentration, which become more pronounced with increasing linear polymer concentration. However, there is no apparent effect of crosslinking density on the morphology of the NIPAAm semi-IPNs. These images are taken after the samples are immersed in MilliQ water to extract any unreacted reagents or linear polymer that has not been trapped in the network. Images taken prior to the extraction step have higher fluorescence intensity but are very similar to these, and the morphology does not appear to be a result of the extraction step.

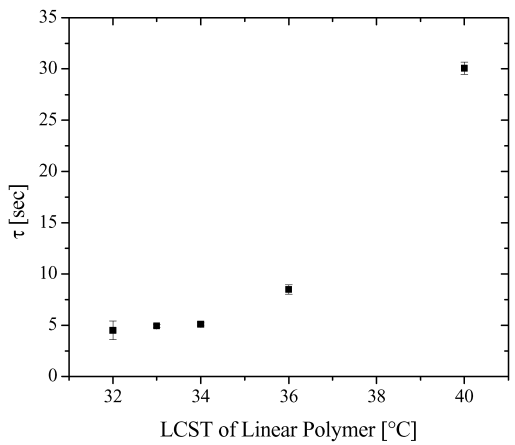


Fig. 4. The time scale $\tau$ as a function of the LCST of the linear polymer. The crosslinked component is NIPAAm, which has an LCST of 32 °C, and the linear polymers are the NIPAAm-*co*-AAm polymers listed in Table 1. Samples are 100 mM of the linear polymer with a crosslinker concentration of 2.1% BIS.

Confocal fluorescence microscopy imaging was also performed on a network containing fluorescein dimethacrylate and a rhodamine-labeled linear polymer, allowing the observation of both the linear and crosslinked components. This double staining experiment is the equivalent of two simultaneous one-photon experiments. The images in Fig. 7 highlight the differences between the AAm and NIPAAm samples. The AAm sample appears to be phase-separated, with the image of the gel network being the negative of the image of the linear polymer. The NIPAAm sample does have regions of higher and lower linear polymer concentration, but this is not related to the morphology of the crosslinked gel network. The separation of the two components in the AAm samples is even more apparent when the images of the linear polymer and crosslinked gel network are overlaid, as shown in Fig. 8. The phase separation of the two components is evident as the dark regions of the crosslinked NIPAAm network (green) correspond to the light regions of the linear AAm component (red). With increased concentration of the linear component, the AAm domains become more interconnected, and this correlates with faster kinetics of the volume phase transition of the corresponding cylindrical samples.

The remaining samples were imaged with conventional (one-photon) confocal fluorescence microscopy using fluorescein-labeled linear polymer. The resulting images (data not shown) show a morphology that is very similar to the NIPAAm samples (see Fig. 6), with regions of higher and lower concentration of linear polymer. These regions range in size from 500 nm to 2 μm and become more pronounced with increased linear polymer concentration, but there is no apparent effect of crosslinking density on the morphology of these semi-IPNs. The samples have a similar morphology, and they also show a monotonic effect of linear polymer concentration on the time scale of response. With the exception of NIPAAm, they also have a slower response with increasing size of the hydrophobic *N*-alkyl group.

Decreasing the molecular weight of the linear polymer does have a small effect on the morphology of the AAm samples, with a larger number of smaller domains for the lower molecular weight linear polymer (see Fig. 9). For example, the 30 mM AAm samples shown have 1.67 ± 0.28 and 1.54 ± 0.24 μm domains for the higher and lower molecular weight linear AAm polymer, respectively. The same comparison for the remaining samples shows no apparent difference in the semi-IPN morphology as a function of the linear polymer molecular weight. The resolution and contrast of conventional confocal fluorescence microscopy and two-photon laser scanning microscopy are different, and there are slight differences in the appearance of the samples with the two imaging techniques (for example, comparing the corresponding images in Fig. 9 with Figs. 5 and 6). However, the sizes and numbers of domains seen for similar samples with the two techniques are consistent, and

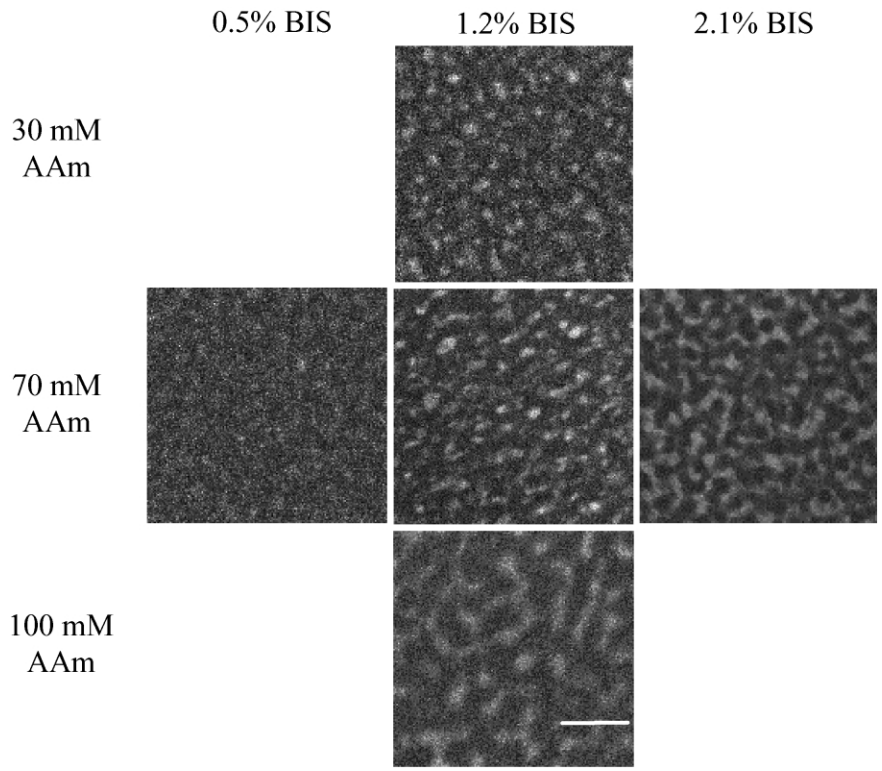


Fig. 5. Two-photon laser scanning microscopy images of a series of AAm semi-IPNs as a function of linear polymer concentration and crosslinker concentration. The linear polymer is labeled with fluorescein isothiocyanate. Scale bar is 5 microns.

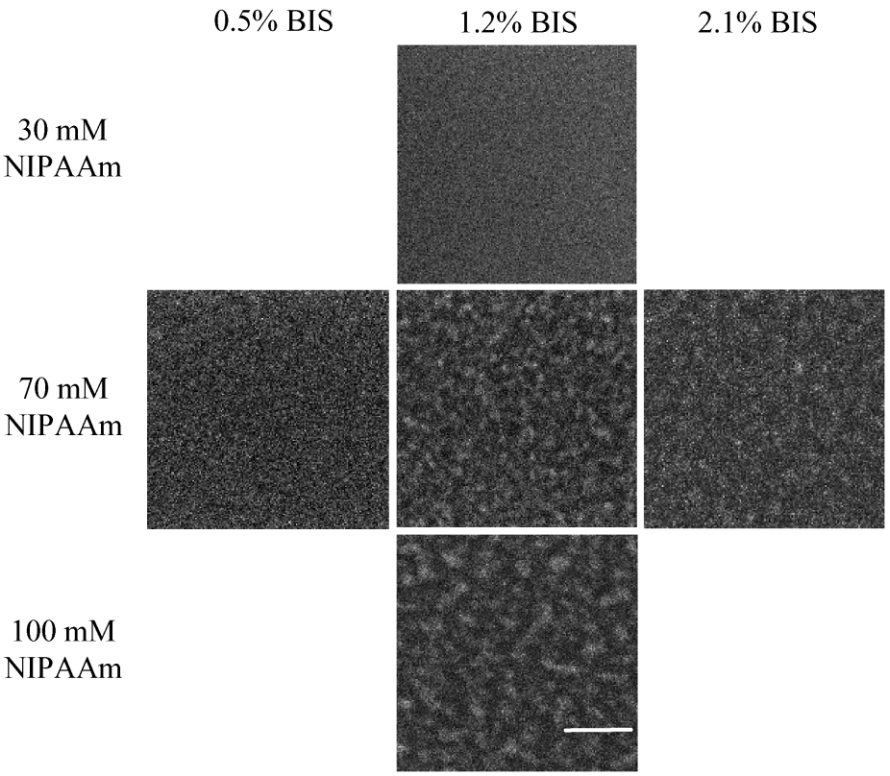


Fig. 6. Two-photon laser scanning microscopy images of a series of NIPAAm semi-IPNs as a function of linear polymer concentration and crosslinker concentration. The linear polymer is labeled with fluorescein isothiocyanate. Scale bar is 5 microns.

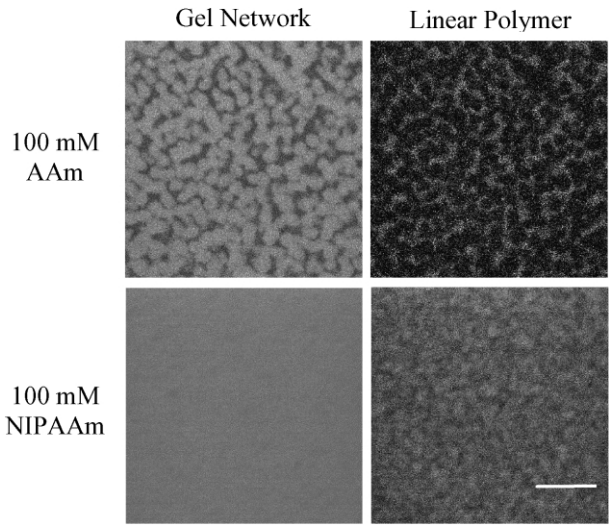


Fig. 7. Double staining confocal microscopy images of AAm and NIPAAm semi-IPNs with 100 mM linear polymer and 1.2% BIS. The linear polymer is labeled with rhodamine B and the crosslinked gel network contains fluorescein dimethacrylate, allowing the two components to be imaged simultaneously. Scale bar is 10 microns.

the data from the two sets of measurements can be compared directly.

## 4. Discussion

Two different confocal microscopy techniques were used to image the internal structures of semi-IPNs based on temperature-responsive NIPAAm hydrogels. We have shown horizontal slices of the two-photon laser scanning microscopy images (see Figs. 5 and 6), but it is also possible to use vertical slices and to reconstruct the entire network. A threshold intensity was chosen as the boundary between the linear and crosslinked domains, and this was used to reconstruct a 3D surface for the linear AAm polymer in the crosslinked matrix. This approach was used to verify that domains shown for the 70 mM AAm/2.1% BIS and the 100 mM AAm/1.2% BIS samples in Fig. 5 are indeed interconnected. The 3D image was displayed with the confocal microscopy software but is not included here due to the difficulty in presenting 3D structures on the printed page. The interconnected linear polymer domains could be interpreted as a percolation threshold, and the fast kinetics seen for these samples can be related to the rapid diffusion of water out of the gel network through interconnected water release channels. This is also an important distinction in considering the previous reports on similar systems that assume a uniform distribution of the linear polymer in the crosslinked NIPAAm network [31–34].

The AAm semi-IPNs are clearly different from the remaining samples, with the characteristic time scale of collapse having a maximum at low concentrations of linear polymer. The imaging of these samples shows that the linear and crosslinked components are phase separated, and the size of the domains is a function of the crosslinking density. The kinetics of the volume phase transition can be correlated to the hydrophilic domains acting as water release channels and becoming more interconnected as a function of crosslinking density as well as linear polymer concentration and molecular weight. A similar mechanism has been proposed for comb-grafted hydrogels, but the resulting domains were too small to be imaged, and no direct comparison could be made. Imaging of the AAm samples with low linear polymer concentration shows individual domains of AAm polymer (see Fig. 8), and this corresponds to the maximum in the time scale of response (see Fig. 2A). As the network collapses, the individual hydrophilic domains may act to trap water within the network and actually impede the diffusion of water out of the core of the gel, with this mechanism being responsible for the maximum in the time scale of response. The remaining samples show no apparent difference as a function of polymer molecular weight and crosslinking density. The regions of higher and lower linear polymer concentration become more pronounced at higher concentrations of linear polymer, but this is not affected by the size of the *N*-alkyl group on the linear polymer. These samples have similar morphology and, with the exception of NIPAAm, a similar effect of the linear polymer composition and concentration on the rate of response.

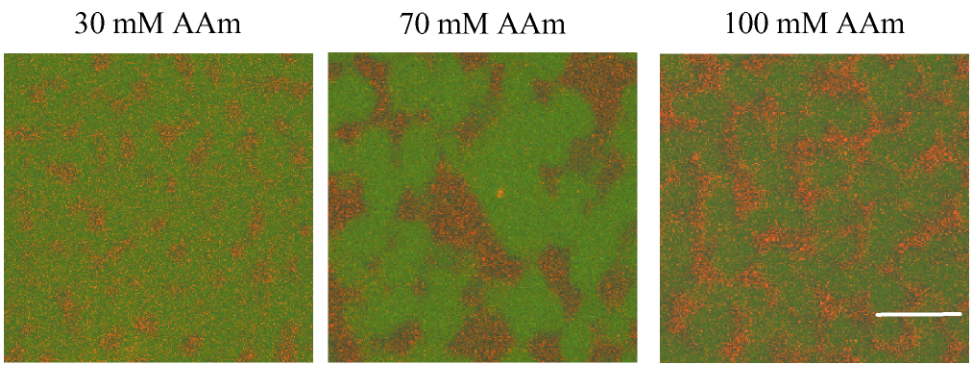


Fig. 8. An overlay of the double staining confocal microscopy images of the linear polymer and the gel network for a series of AAm semi-IPNs. The samples all have a crosslinker concentration of 1.2% BIS with linear polymer concentrations as shown. The linear polymer is labeled with rhodamine B (red) and the crosslinked gel network contains fluorescein dimethacrylate (green). Scale bar is 5 microns.

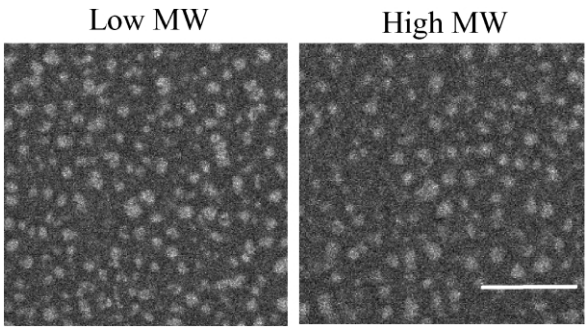


Fig. 9. Confocal microscopy images showing the effect of molecular weight on AAm semi-IPNs with 30 mM linear polymer and 1.2% BIS. The linear polymers are labeled with fluorescein isothiocyanate. Scale bar is 10 microns.

The NIPAAm samples do have much faster kinetics than expected, but this series of samples is unique in that the linear polymer and the crosslinked network have the same LCST and respond simultaneously to the step change in temperature. This effect was further probed by using a series of NIPAAm-*co*-AAm linear polymers, with increased LCST as a function of increasing AAm concentration. The resulting semi-IPNs had a linear component with an LCST greater than that of the crosslinked NIPAAm component. In response to an increase in temperature, the linear component should therefore respond after the crosslinked component, and the response of the resulting semi-IPN is slower (see Fig. 4). The DEAAm samples have a linear component with an LCST lower than that of the crosslinked NIPAAm component, and the resulting response is also slower (see Fig. 3). This supports the idea that the fast response of the NIPAAm samples (see Fig. 4) is due to the linear and crosslinked components having the same LCST and responding simultaneously to the step change in temperature. However, there is no reason to assume that the behavior for linear components with an LCST above that of the crosslinked component is the same as for linear components with an LCST below that of the crosslinked component. In other words, the mechanism of the slow response of the DEAAm semi-IPNs is not necessarily the same as for the NIPAAm-*co*-AAm10 samples. Thus, this system needs to be studied in greater detail for a complete understanding of this effect.

These results suggest that cooperative motion of the linear and crosslinked components will result in uniform collapse of the responsive network and faster kinetics of the volume phase transition. The higher mobility of the linear polymers allows hydrophobic aggregation to occur throughout the network, and the effects of NIPAAm molecular weight on the kinetics can be related to the increased mobility of the lower molecular weight linear polymers. This does not explain the faster kinetics with higher crosslinking density, but it is possible that the higher mobility of the linear polymer becomes even more important in the collapse of a more rigid network with higher crosslinking density.

## 5. Conclusion

The kinetics of the volume phase transition was studied for a series of fast-responsive semi-IPNs based on NIPAAm as the crosslinked component and a series of *N*-alkyl-substituted acrylamides as the linear component. The same series of samples was fluorescently labeled and imaged using confocal fluorescence microscopy and two-photon laser scanning microscopy, and the morphology of the semi-IPNs was used to explain the mechanism of the faster kinetics. The most hydrophilic of the linear polymers appears to be phase separated, and the kinetics of the volume phase transition can be related to the appearance of interconnected hydrophilic domains within the responsive crosslinked network. The morphology of the remaining samples is not clearly related to the corresponding kinetics, but the fast kinetics of the NIPAAm linear polymer in a crosslinked NIPAAm matrix suggests that the effect is primarily due to the simultaneous collapse of the two components of the semi-IPNs. Previous reports on similar systems have taken a more quantitative approach, assuming uniform distribution of the linear polymers in the crosslinked hydrogel network. With confocal microscopy we have shown that this is clearly not the case, and the resulting images correlate well with the kinetics of the semi-IPN volume phase transition.

## Acknowledgements

This work was supported by an NSF Graduate Research Fellowship (M.E.H.), the Center on Polymer Interfaces and Macromolecular Assemblies (CPIMA), which was sponsored by the NSF-MRSEC program under DMR 9808677, and the NSF XYZ-on-a-chip program under DMR 9980799.

## References

[1] Tanaka T, Fillmore D, Sun ST, Nishio I, Swislow G, Shah A. Phys Rev Lett 1980;45:1636–9.
[2] Eichenbaum GM, Kiser PF, Simon SA, Needham D. Macromolecules 1998;31:5084–93.
[3] Shiga T. Adv Polym Sci 1997;134:131–63.
[4] Juodkazis S, Mukai N, Wakaki R, Yamaguchi A, Matsuo S, Misawa H. Nature (London) 2000;408:178–81.
[5] Suzuki A, Ishii T. J Chem Phys 1999;110:2289–96.
[6] Peppas NA, Langer R. Science (Washington, DC) 1994;263:1715–20.
[7] Peppas NA, Huang Y, TorresLugo M, Ward JH, Zhang J. Annu Rev Biomed Engng 2000;2:9–29.
[8] Schild HG. Prog Polym Sci 1992;17:163–249.
[9] Matsuo ES, Tanaka T. J Chem Phys 1988;89:1695–703.
[10] Gan DJ, Lyon LA. J Am Chem Soc 2001;123:7511–7.
[11] Kuckling D, Harmon ME, Frank CW. Macromolecules 2002;35:6377–83.
[12] Gemeinhart RA, Chen J, Park H, Park K. J Biomater Sci, Polym Edn 2000;11:1371–80.
[13] Kato N, Takahashi F. Bull Chem Soc Jpn 1997;70:1289–95.

[14] Kabra BG, Gehrke SH. Polym Commun 1991;32:322–3.
[15] Zhang XZ, Yang YY, Chung TS, Ma KX. Langmuir 2001;17:6094–9.
[16] Kaneko Y, Nakamura S, Sakai K, Aoyagi T, Kikuchi A, Sakurai Y, Okano T. Macromolecules 1998;31:6099–105.
[17] Kaneko Y, Sakai K, Kikuchi A, Yoshida R, Sakurai Y, Okano T. Macromolecules 1995;28:7717–23.
[18] Kobiki Y, Suzuki A. Int J Adhes Adhes 1999;19:411–6.
[19] Suzuki A, Yamazaki M, Kobiki Y. J Chem Phys 1996;104:1751–7.
[20] Zhang J, Peppas NA. J Biomater Sci: Polym Edn 2002;13:511–25.
[21] Matzelle TR, Ivanov DA, Landwehr D, Heinrich LA, Herkt-Bruns C, Reichelt R, Kruse N. J Phys Chem, B 2002;106:2861–6.
[22] Hirokawa Y, Jinnai H, Nishikawa Y, Okamoto T, Hashimoto T. Macromolecules 1999;32:7093–9.
[23] Tokita M, Suzuki S, Miyamoto K, Komai T. J Phys Soc Jpn 1999;68:330–3.
[24] Sperling LH, Mishra V. Polym Adv Technol 1996;7:197–208.
[25] Elisseeff J, McIntosh W, Anseth K, Riley S, Ragan P, Langer R. J Biomed Mater Res 2000;51:164–71.
[26] Ramaraj B, Radhakrishnan G. J Appl Polym Sci 1994;51:979–88.
[27] Park YJ, Liang JF, Yang ZQ, Yang VC. J Controlled Release 2001;75:37–44.
[28] Eschbach FO, Huang SJ. Adv Chem Ser 1994;239:205–19.
[29] Wang MZ, Qiang JC, Fang Y, Hu DD, Cui YL, Fu XG. J Polym Sci, Part A: Polym Chem 2000;38:474–81.
[30] Kayaman-Apohan N, Baysal BM. Macromol Chem Phys 2001;202:1182–8.
[31] Shin BC, Jhon MS, Lee HB, Yuk SH. Eur Polym J 1998;34:171–4.
[32] Zhai ML, Li J, Yi M, Ha HF. Radiat Phys Chem 2000;58:397–400.
[33] Hirotsu S. Jpn J Appl Phys, Part 2 1998;37:L284–7.
[34] Harmon ME, Frank CW. ACS Symp Ser 2002;833:2–11.
[35] Abetz V, Meyer GC, Mathis A, Picot C, Widmaier JM. Polym Adv Technol 1996;7:295–302.
[36] Brandrup J, Immergut EH. Polymer handbook. New York: Wiley; 1989.
[37] Plate NA, Lebedeva TL, Valuev LI. Polym J 1999;31:21–7.
[38] Hermanson GT. Bioconjugate techniques. San Diego: Academic Press; 1996.
[39] Harmon ME, Jakob TAM, Knoll W, Frank CW. Macromolecules 2002;35:5999–6004.
[40] Kaneko Y, Nakamura S, Sakai K, Kikuchi A, Aoyagi T, Sakurai Y, Okano T. Polym Gels Networks 1998;6:333–45.
[41] Inoue T, Chen GH, Nakamae K, Hoffman AS. Polym Gels Networks 1997;5:561–75.